Electrical discharges in the Reverse Vortex Flow – Tornado Discharges

Chiranjeev S. Kalra, Mikhail Kossitsyn, Kamilla Iskenderova, Alexandre Chirokov,
Young I. Cho, Alexander Gutsol, Alexander Fridman

Drexel University, College of Engineering, Drexel Plasma Institute

Abstract:

Properties of the electrical discharges in the Reverse Vortex Flows (Tornado Discharges - TD) differ significantly from the prosperities of discharges in the flows of conventional geometries. This difference is the most considerable for the non-equilibrium discharges. The reason of the difference is an intensive convective cooling of the discharge zone and a perfect thermal insulation of the discharge zone from the walls. This difference makes TD very attractive for many applications.

1. Introduction

It is relatively easy to realize the Reverse Vortex Flow (RVF), which is very similar to the natural tornado, in the cylindrical volume. It is necessary to direct an outlet of the flow from the volume along the axis to the swirl generator side, and the diameter of the outlet should be considerably less than that of the cylindrical vessel (Fig. 1).

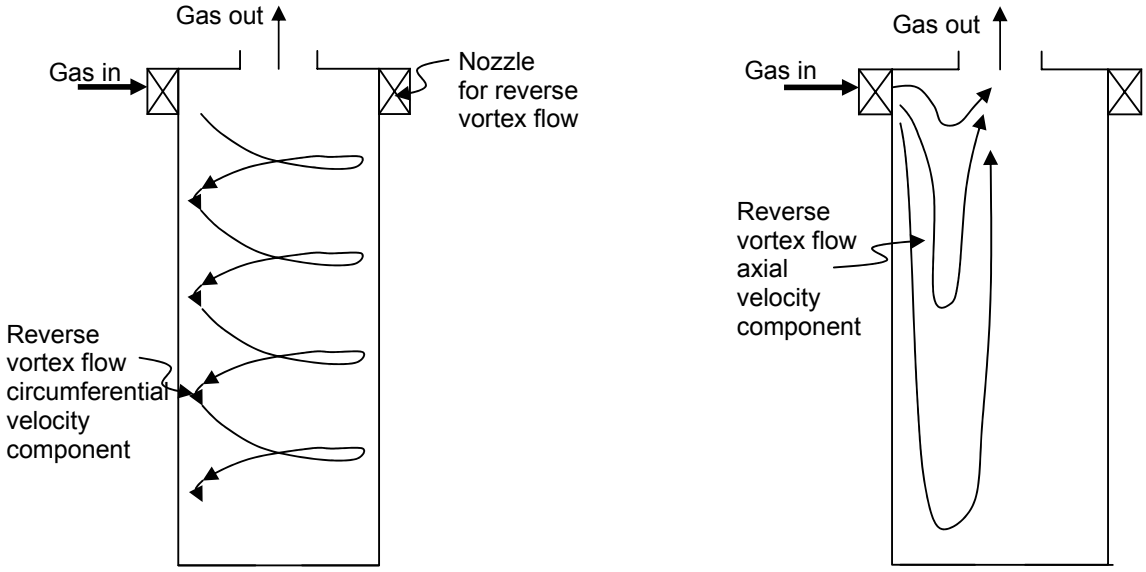

Figure 1: Reverse Vortex ("Tornado") flow in a cylindrical reactor.

Several kinds of atmospheric pressure electrical discharges were already realized in the RVF: microwave (MW) discharge [1 - 6], RF ICP [6 - 9], arc and gliding arc. Gaseous flame, which could be also considered as low temperature plasma, was also realized in tornado geometry [5, 10 - 14]. In the cases of MW and RF ICP plasma generators and gas combustion chamber, the RVF have been compared experimentally (calorimetric investigations) and numerically with conventional "forward" vortex flow (FVF). Here we present some new results regarding simulation of RF ICP generator and experiments with arc and gliding arc in RVF, and discuss all obtained results from the unified point of view.

2. Self-consistent simulation of RF ICP generator with Reverse Vortex Flow

Argon ICP generator with RVF was studied experimentally earlier [7 - 9]. Also we have published already the results of simplified simulation of this generator [6 - 8], where gas-dynamic problem was solved in assumption about place and size of energy release zone. Today we have and present results of self-consistent modeling. Plasma is assumed to be in local temperature equilibrium and optical thin.

Electromagnetic field calculation was based on a current loop method. Consider a cylindrical loop of radius *R* carrying a current *I*, as shown on a Fig.1. The vector potential will be equal to $A_\theta(r,z) = \frac{\mu_0 I}{2\pi}\sqrt{\frac{R}{r}}G(k)$

Where

$$G(k) = \frac{(2-k^2)K(k) - 2E(k)}{k}$$

$$k^2 = \frac{4Rr}{(R+r)^2 + (z-z_c)^2}$$

K and *E* are the complete elliptic integrals.

Therefore, the electromagnetic field can be calculated from these equations:

$$A_R(r,z) = \frac{\mu_0 I}{2\pi}\sqrt{\frac{R}{r}}\sum_{i=1}^{coil} G(k_i) + \frac{\mu_0 \omega}{2\pi}\sum_{i=1}^{C.V.}\sqrt{\frac{r_i}{r}}\sigma_i A_{I,i} S_i G(k_i)$$

$$A_I(r,z) = -\frac{\mu_0 \omega}{2\pi}\sum_{i=1}^{C.V.}\sqrt{\frac{r_i}{r}}\sigma_i A_{R,i} S_i G(k_i)$$

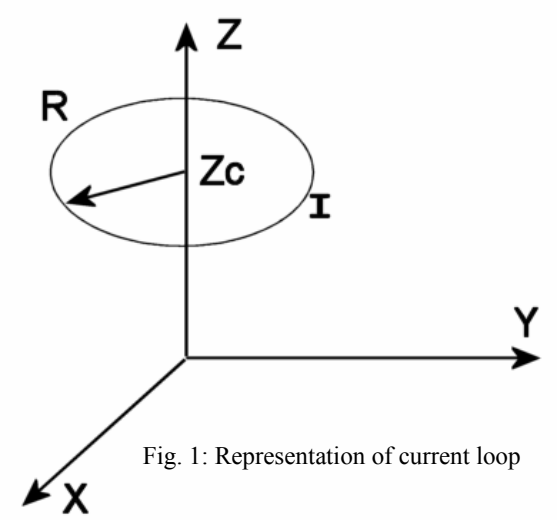

Fig. 1: Representation of current loop

These equations were solved by successive iterations to get real and imaginary part of vector potential. Lorenz force, *F*, and local energy dissipation rate, *P*, were calculated using vector potential [15]. We assumed radiation losses are the function of the local temperature [16]. Gas flow coupled together with electromagnetic field equations was solved by FLUENT (Version 6) in axially symmetric 2D case. Build-in Reynolds Stress turbulence model was employed. The coupling scheme is shown on a Fig.2.

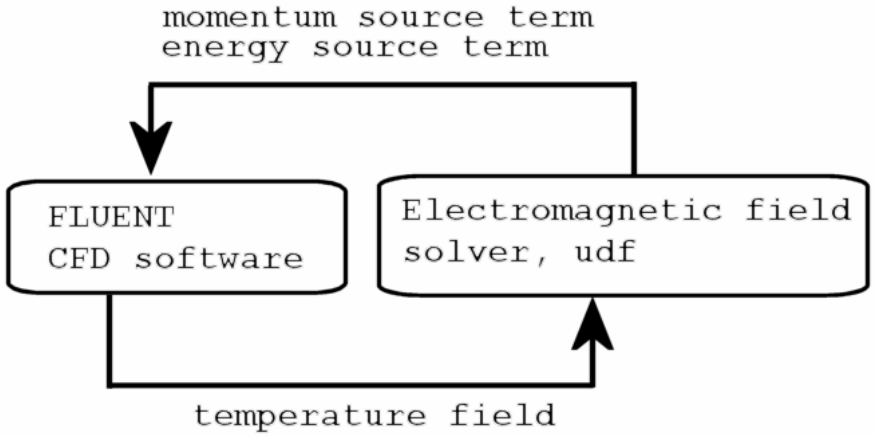

Figure 2: Coupling framework

Results of simulation are in a good agreement with experimental data obtained previously (Fig. 3). If we compare the results of self-consistent simulation with the results of simplified simulation of this generator [6 - 8], it is possible to see that the main difference is larger diameter of the energy release zone (heating zone). Convergence of self-consistent simulation was obtained with plasma only for the cases with low efficiency (Fig. 4, the temperature fields for the cases marked by red circles in Fig. 3), where the recirculation zone near the closed end of the generator still exists. This recirculation zone formed because of Ampere force, results in formation of the central plasma "tail" (Fig. 3a) of disturbance of the temperature field (Fig.3b). Attempts to simulate more efficient regimes (with lower power or higher flow rates) results in going out of plasma (temperature of the plasma drops, consequently conductivity drops and power absorption drops too). It was possible to improve the situation by assuming that conductivity depends not only on gas temperature but on electric field also (assumption of non-equilibrium). This assumption results in better agreement with the experiments but permits to move into the higher flow rates very little, then plasma goes out again. We suppose that in experiments we have diffusion of electrons to the outer layer of

plasma, and there conductivity is much higher then that in assumption of equilibrium or temperature dependence. Probably it is possible to simulate this in two-liquid assumption (electron gas and argon should be considered separately along with ambipolar diffusion). Such simulation is in our plans for future.

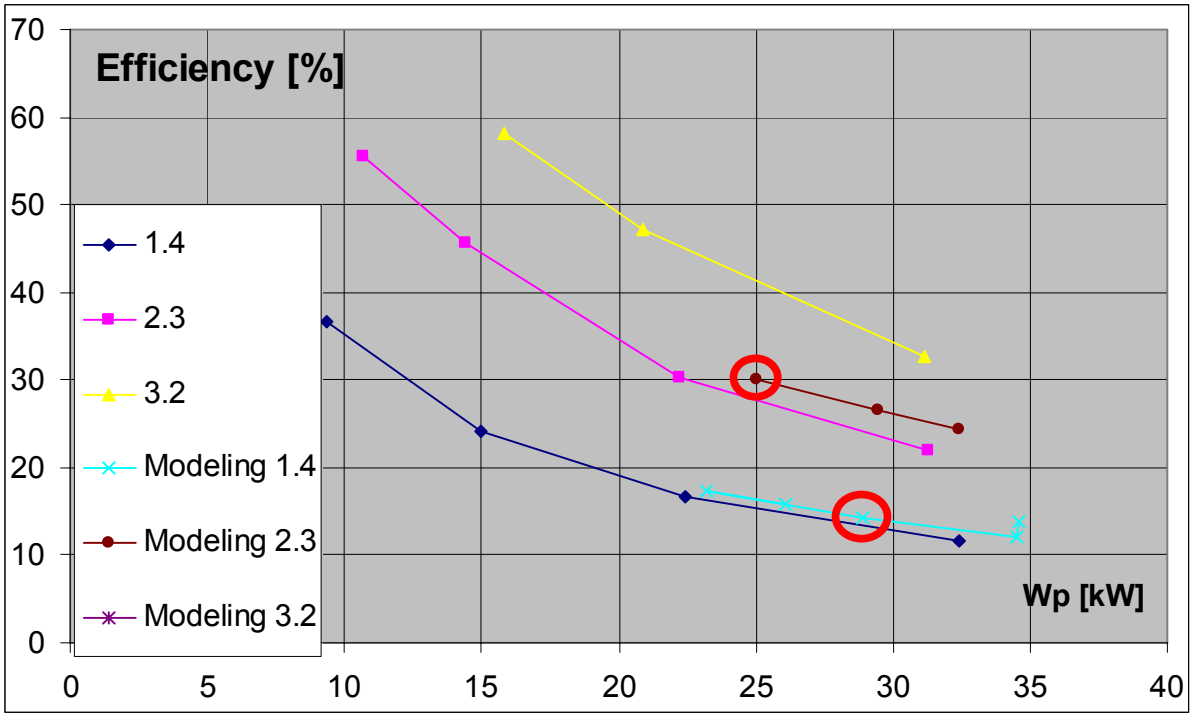

Figure 3: Comparison between the experimental data [9] and simulation for three levels of argon flow rate 1.4, 2.3 and 3.2 g/s. Red circles mark the points presented in Fig. 4.

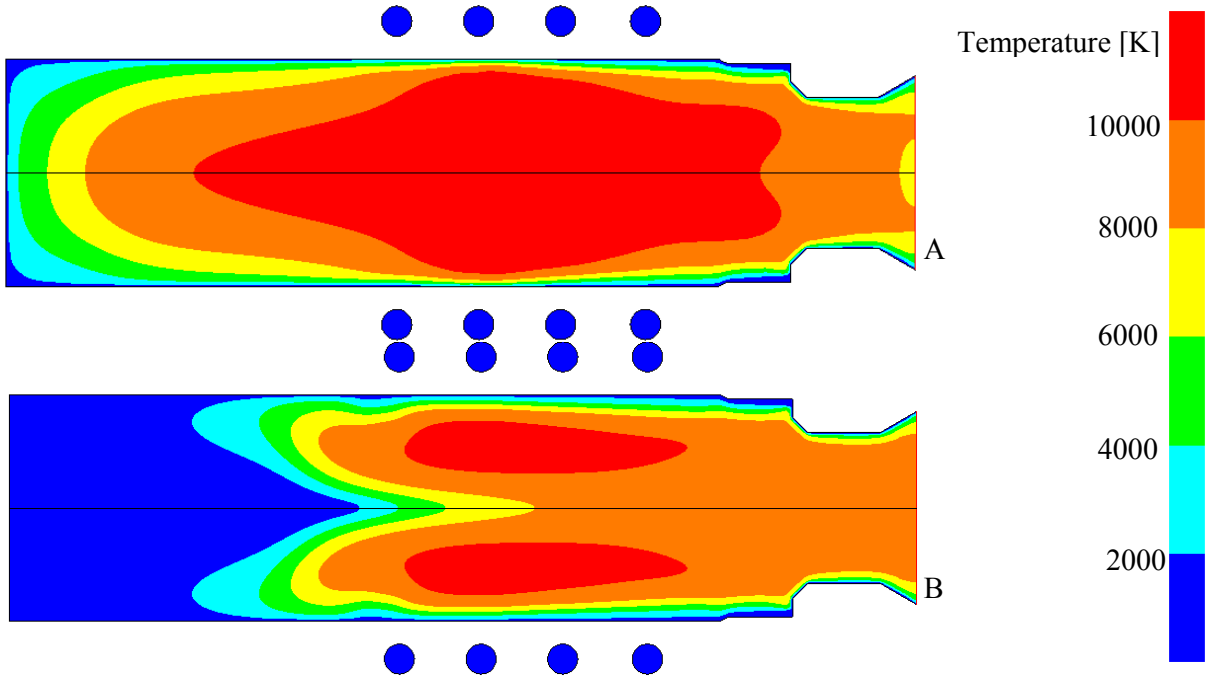

Figure 4: Temperature field for two simulated cases marked by red circles in Fig. 3: (A) – 1.4 g/s of argon and 28 kW of plasma power; (B) – 2.3 g/s of argon and 25 kW of plasma power.

3. Experiments with arc and gliding arc in Reverse Vortex Flow

Conventional gliding arc is a high-pressure gas non-stationary discharge [17, 18]. The arc starts in a narrow gap between two or more diverging electrodes in a gas flow, after breakdown when the electric field in this gap reaches approximately 3 kV/mm in air. The arc current increases very fast and the voltage on the arc drops. If gas flow is strong enough, it forces the arc to move along the diverging electrodes and elongate. The growing arc demands more power to sustain itself. It continues to elongate till the power supply can no longer compensate the energy lost in heat transfer to the surrounding gas. The arc cools down and finally extinguishes. The next cycle starts immediately after the voltage reaches the breakdown value, usually just after fading of the previous arc.

The gliding arc can operate in non-equilibrium regimes and have relatively low gas temperatures [17, 18]. Previously gliding arc has been reported for applications in the field of plasma-catalytic conversion of organic compounds, etc [19, 20]. Gliding arc requires velocities high enough to move the discharge along diverging electrodes but plasma catalytic conversions require high residence time for higher degree of completion of chemical reactions. Specific power delivered remains low in case of non-equilibrium regime and conventional (flat, in the case of two electrodes) geometry. Also a large amount of gas passes around the arc resulting in no residence in the discharge zone. Thus the gliding arc looks to have potentially a number of application and attractive for plasma-catalytic conversions but unable to give expected results. That is why we use a new approach to get gliding in circular geometry in the reverse vortex flow.

Gliding Arc in Tornado works in a Reverse Vortex Flow setup in a cylindrical volume (ϕ 40mm; L=150mm) (Fig. 5). A circular and spiral electrode is placed in the plane of the flow near the cylinder walls. The flow conditions and the characteristics of the power supply determine the shape of the spiral electrode. Based on experimental flow visualization and numerical modeling of the flow conditions the spiral shape and characteristics are determined. The voltage, 10 kV, from Voltronics power supply gives power as high as 2.5 kW per discharge in laboratory experiments.

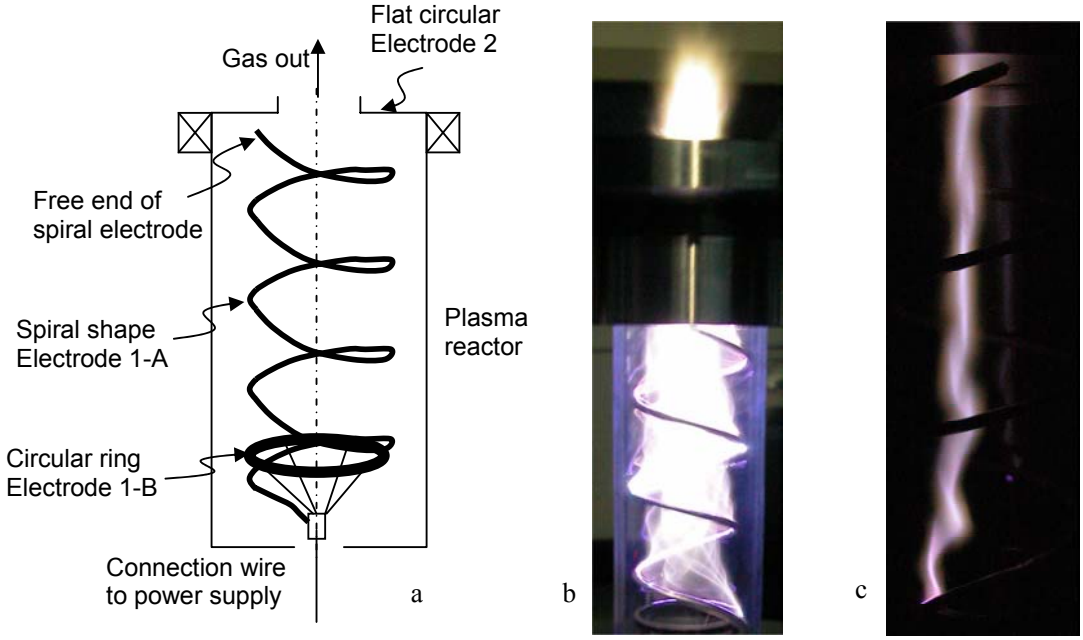

Figure 5: Tornado Gliding Arc (TGA), a – schematic of TGA reactor; b - photo image of gliding arc with normal exposition time; c - photo image of gliding arc with shot exposition time (1/1000 s).

The reactor as shown in the figure 5a essential consists of a cylindrical volume, with metal flange at the outlet. This metal flange at the outlet also acts as anode and is connected to the ground terminal. The flange also houses 4 tangential inlets into the cylindrical tube. Gas enters through these tangential inlets (2mm x 2mm) into the tube generating a strong reverse vortex inside. Typical inlet velocities vary from 10m/s to 50m/s. An additional axial inlet is provided to add more gas flow for additions of reactants in case of plasma-catalytic conversions. The spiral electrode is connected axially in the tube and acts as the cathode. The end of

the spiral turns to form a ring smaller in diameter than the spiral itself. In fact the diameter of the spiral goes on decreasing as it moves away from the anode.

When high potential is applies across the electrodes (about 3kV/mm in air) electrical breakdown ignites the gliding arc. The strong vortex flow forces this arc to move around the tube axis. The arc thus elongates along the spiral. Eventually the elongated arc reaches the ring shaped end of the spiral electrode (Fig. 5b and Fig 6. In the second case the discharge was formed by elongating the distance between two electrodes). Now the arc is in the central zone of the reactor, this zone has relatively less disturbances. This is the central discharge zone or the center column.

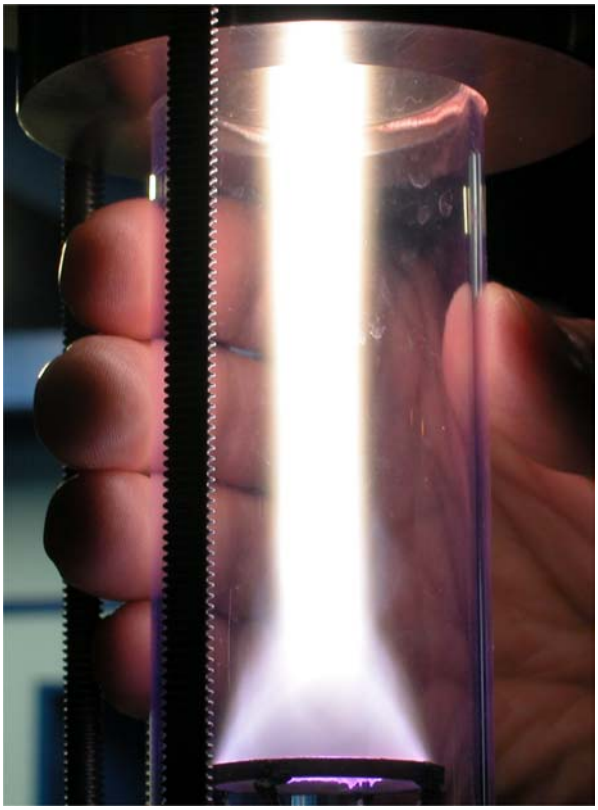

Figure 6: Tornado Gliding Arc (TGA) between circular electrode and flange (flat circular electrode).

The discharge zone has very intensive convective cooling due to the vortex flow around it and the central flow through it. At the same time this discharge zone because of the same vortex flow is in perfect thermal insulation form the reactor wall (Fig. 6). Very fast movement of the electrode spots results in no electrode erosion or deterioration. The elongation of the arc in this case is not due to the shape of the electrodes, instead the arc moves on two parallel electrodes. This elongation is due to the different velocities of the gas flowing near the electrodes (Fig. 7). Due to this the arc elongates and finally reaches a point where the thermal losses due to elongation of the arc can no longer be compensated by the power supply. At this point the plasma supported re-ignition of the arc is observed. This is possible because of the circular geometry.

Figure 7: Elongation of arc on parallel electrodes but with different gas flow velocities near the two electrodes

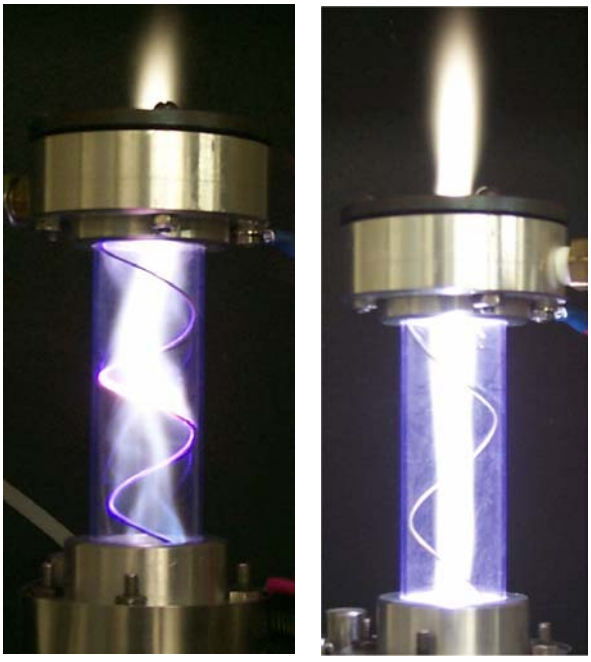

Figure 8: Tornado Gliding Arc (left) may transform to the high voltage atmospheric pressure discharge inside the Reverse Vortex Flow (right).

It is also possible to stabilize the ordinary arc in RVF. Fig. 8 demonstrates transformation of the TGA to the high voltage atmospheric pressure discharge inside RVF.

4. Discussion and Conclusion

Perfect thermal insulation properties of RVF were emphasized earlier [1 - 14]. Here we'd like to emphasize the influence of convective cooling of the central zone on the plasma properties. Between thermal plasmas (arcs, ICP) and cold plasmas (DBD, corona) of atmospheric pressure it is a range where relatively hot non-equilibrium (transitional) plasmas

exist. Such kind of plasmas can be realized in the case of microwave discharge or gliding arc [21]. In transitional plasmas electric field is relatively strong, translational and electron temperatures are strongly coupled and changes together [12]. Decrease of translational temperature results in increase of plasma electric field and electron temperature, and plasma becomes more non-equilibrium. This effect can be easily realized in the reverse vortex flows because of intensive convective cooling of central zone by turbulence and axial flow (see Fig. 4B for example). The first example of such effect is the temperature drop (at least according to simulation) in the Reverse Vortex Stabilized microwave discharge [2 - 5]. Gliding Arc and High Voltage atmospheric Pressure Discharge in RVF is another example. In RVF gliding arc exists in conditions corresponded to extremely elongated gliding arc between two divergent electrodes, means in the most non-equilibrium state [18, 21]. In contrast to conventional thermal and non-thermal discharges, the transitional discharges are able to provide simultaneously high plasma density, power and operating pressure (typical for thermal systems) with high level of non-equilibrium, high electron temperature, low gas temperature and possibility of stimulation selective chemical processes without any quenching (typical for non-thermal systems). That is why transitional discharges in the Reverse Vortex Flows and Tornado Gliding Arc particularly, combining high extent of non-equilibrium with high residence time, are very attractive for many applications.

References:

[1] V. T. Kalinnikov and A. F. Gutsol - Doklady Akademii Nauk, 1997, V. 353 (4), p. 469-471. (Physics - Doklady, Vol. 42, No. 4, 1997, pp. 179 - 181).
[2] A. Gutsol, J. A. Bakken - ISPC-13, Beijing, China, Aug.18-22, 1997. Vol. 1, p. 155-160.
[3] A. Gutsol, J. A. Bakken - J.Physics D: Applied Physics , 1998 , V. 31, No. 6, pp. 704 - 711.
[4] A. Gutsol, J. A. Bakken - In: Thermal Plasma Torches and Technologies. Edited by O. P. Solonenko. Vol. 1. Plasma Torches: Basic Studies and Design. CISP, Cambridge, England. 1998.
[5] A. Gutsol, A. Fridman, L. Kennedy – HEFAT- 2002: 1st International Conference on Heat Transfer, Fluid Mechanics, and Thermodynamics, Kruger Park, South Africa, 2002. Vol. II, pp. 987 – 992.
[6] A. Chirokov, A. Gutsol, A. Fridman, L. Kennedy – ISPC-15, Orleans, 2001, Vol. I, pp. 167 – 172.
[7] A. Gutsol, J. Larjo, R. Hernberg – ISPC-14, Prague, 1999, Vol. 1, pp. 227 - 231.
[8] A. Gutsol, J. Larjo, R. Hernberg - Teplofizika vysokikh temperatur, Vol. 39, No. 2, 2001, pp. 187-197. (High Temperature, Vol. 39, No. 2, 2001, pp. 169 - 179.)
[9] A. Gutsol, J. Larjo, R. Hernberg - Plasma Chem. and Plasma Proc., Vol. 22, No. 3, 2002, p. 351-369.
[10] V. T. Kalinnikov and A. F. Gutsol - Doklady Akademii Nauk, 1998, V. 360 (1), p. 49-52. (Physics - Doklady, Vol. 43, No. 5, 1998, pp. 302 - 305).
[11] V. T. Kalinnikov and A. F. Gutsol Reverse - Teplofizika vysokikh temperatur, Vol. 37, No. 2, 1999, pp. 194 - 201. (High Temperature, Vol. 37, No. 2, 1999, pp. 172 - 179.)
[12] A. F. Gutsol - Matematicheskoe modelirovanie (Math. Modeling), 1999. V. 11. No. 6. pp. 38 – 44.
[13] A. Gutsol - In: Progress in Plasma Processing of Materials 1999. Editors: Pierre Fauchais and Jacques Amouroux. Begell House, Inc., NY, 1999. P. 81 - 86.
[14] A. Gutsol, A. Fridman, L. Kennedy – 29th Int. Symp. on Combustion, Sapporo, Japan, July 21-26, 2002, Abstract 1-14-1065, p. 92.
[15] J. Mostaghimi, M. I. Boulos - Plasma Chem. and Plasma Proces., Vol. 9, 1, (1989).
[16] T.G. Owano, M.H. Gordon, C.H. Kruger - Phys. Fluids, B 2 (12), (1990).
[17] I. Kuznetsova, N. Kalashnikov, A. Gutsol, A. Fridman, L. Kennedy – ISPC-15, Orleans, 2001. Vol. IV, pp. 1509 - 1514.
[18] I. Kuznetsova, N. Kalashnikov, A. Gutsol, A. Fridman, L. Kennedy – Journal of Applied Physics, 2002, V. 92, No. 8, pp. 4231-4237.
[19] A. Czernichowski - Pure & Appl. Chem. **66(**6), pp. 1301-1310 (1994)
[20] K. Iskenderova, P. Porshnev, A. Gutsol, A. Saveliev, A. Fridman, L. Kennedy, T. Rufael – ISPC-15, Orleans, 2001. Vol. VII, pp. 2849 - 2854.
[21] M. Kossitsyn, A. Gutsol, A. Fridman - ISPC-16, Taormina, Italy, 2003.